Petroleum Science 21 (2024) 1944–1954

Contents lists available at ScienceDirect

Petroleum Science

journal homepage: www.keaipublishing.com/en/journals/petroleum-science

Original Paper

Influences of shale microstructure on mechanical properties and bedding fractures distribution

Ming-Zhe Gu [a, b], Mao Sheng [a, b, *], Shi-Zhong Cheng [a, b], Fan-Hao Gong [c, **], Gen-Sheng Li [a, b]

[a] State Key Laboratory of Petroleum Resources and Engineering, China University of Petroleum-Beijing, Beijing, 102249, China
[b] College of Petroleum Engineering, China University of Petroleum-Beijing, Beijing, 102249, China
[c] Shenyang Center of China Geological Survey, Shenyang, Liaoning, 110034, China

ARTICLE INFO

Article history:
Received 6 June 2023
Received in revised form
17 July 2023
Accepted 8 November 2023
Available online 13 November 2023

Edited by Jie Hao and Teng Zhu

Keywords:
Shale
Nanoindentation
Microstructure
Mechanical property
Fracture

ABSTRACT

The difference in microstructure leads to the diversity of shale mechanical properties and bedding fractures distribution patterns. In this paper, the microstructure and mechanical properties of Longmaxi marine shale and Qingshankou continental shale were studied by X-ray diffractometer (XRD), field emission scanning electron microscope (FE-SEM) with mineral analysis system, and nanoindentation. Additionally, the typical bedding layers area was properly stratified using Focused Ion Beam (FIB), and the effects of microstructure and mechanical properties on the distribution patterns of bedding fractures were analyzed. The results show that the Longmaxi marine shale sample contains more clay mineral grains, while the Qingshankou continental shale sample contains more hard brittle mineral grains such as feldspar. For Longmaxi marine shale sample, hard brittle minerals with grain sizes larger than 20 μm is 18.24% and those with grain sizes smaller than 20 μm is 16.22%. For Qingshankou continental shale sample, hard brittle minerals with grain sizes larger than 20 μm is 40.7% and those with grain sizes smaller than 20 μm is 11.82%. In comparison to the Qingshankou continental shale sample, the Longmaxi marine shale sample has a lower modulus, hardness, and heterogeneity. Laminated shales are formed by alternating coarse-grained and fine-grained layers during deposition. The average single-layer thickness of Longmaxi marine shale sample is greater than Qingshankou continental shale sample. The two types of shale have similar bedding fractures distribution patterns and fractures tend to occur in the transition zone from coarse-grained to fine-grained deposition. The orientation of the fracture is usually parallel to the bedding plane and detour occurs in the presence of hard brittle grains. The fracture distribution density of the Longmaxi marine shale sample is lower than that of the Qingshankou continental shale sample due to the strong heterogeneity of the Qingshankou continental shale. The current research provides guidelines for the effective development of shale reservoirs in various sedimentary environments.

1. Introduction

Complex sedimentary environments differentiate continental shale from marine shale in petrophysical and geochemical properties (Li et al., 2018). The development techniques of marine shale are not fully applicable to continental shale. Understanding the characteristics of various types of shale reservoirs is crucial for enhancing the efficient development and technological preference of shale oil and gas (Huo et al., 2018; Wei et al., 2018; Wang et al., 2019; Yang and Liu, 2021).

Many researchers have examined the disparities in shale properties in various sedimentary environments. Jiang et al. (2016) investigated marine shale, transitional shale, and lacustrine shale to compare and analyze the reservoir characteristics and hydrocarbon generation potential in different sedimentary environments. Yang et al. (2018) examined the impacts of TOC and other factors on the wettability of marine shale and continental shale.

* Corresponding author.
** Corresponding author.
E-mail addresses: shengmao@cup.edu.cn (M. Sheng), gfh1004@163.com (F.-H. Gong).

https://doi.org/10.1016/j.petsci.2023.11.012

Chen et al. (2019) and Xie et al. (2021) compared the differences in pore structure and controlling factors in various diagenetic stages of marine shale, transitional shale, and continental shale using field emission scanning electron microscope (FE-SEM), high-pressure mercury compression, and other techniques. Using thin section identification and methane adsorption, Xiao et al. (2021) studied the difference in gas content and gas storage mechanism between marine shale and continental shale.

At present, the primary methods for evaluating the mechanical properties of shale reservoirs are mainly uniaxial and triaxial mechanical experiments (Mokhtari et al., 2016; Li et al., 2019; Cao et al., 2020; Wang et al., 2020a; Jia et al., 2021) and ultrasonic velocity measurement (Gong et al., 2018; Ding et al., 2021; Lawal et al., 2021) of shale outcrops, however, there is not enough information in characterizing the mechanical properties of real reservoirs. As one of the rapidly developing mechanical testing techniques in recent years, nanoindentation has effectively characterized the nanoscale mechanical properties of downhole cores. Chen et al. (2015) and Dong and Chen (2017) used nanoindentation to obtain the hardness and elastic modulus of Longmaxi shale, as well as the relationship between the loading rate and critical fracture load of the shale. Liu et al. (2016) determined the mechanical properties of Bakken shale with various mineral fractions at the nanoscale and demonstrated that the fracture toughness of the specimens was proportional to Young's modulus. Liu et al. (2022b) examined the mechanical properties of typical minerals in shales and analyzed the formation mechanisms of radial and shear fractures. Li et al. (2023) obtained the evolution of the degree of shale softening through nanoindentation by varying the soaking time of water/CO_2 on the Shahejie shale. However, most of the previous studies on the mechanical properties of shale have been conducted on a single sedimentary environment, without the evaluation of the effects of different microstructures on the mechanical properties and bedding fractures distribution.

In this paper, the Longmaxi marine shale sample and Qingshankou continental shale sample were examined using the X-ray diffractometer (XRD), field emission scanning electron microscope (FE-SEM), and nanoindentation lattice. Those two shale samples' microstructure and mechanical properties were quantitatively analyzed. In addition, the Focused Ion Beam (FIB) technique was used to accurately stratify the selected typical bedding layer areas, the mechanical properties of each layer were characterized and the bedding fractures distribution in laminated shale were discussed. This study plays a crucial guiding role in the targeted development of oil and gas from shale.

2. Materials and methods

2.1. Material and specimen preparation

The marine and continental downhole cores were collected from the Lower Silurian Longmaxi Formation and the Upper Cretaceous Qingshankou Formation, respectively, with vertical burial depths of 4059 m and 2113 m. As shown in Fig. 1, the downhole shale cores are cylindrical and the bedding plane directions are perpendicular to the sample axis. The 10 mm length × 5 mm width × 5 mm height cubes were extracted from each of the two shale samples along the axis direction with a waterless wire-cutting technique to eliminate water saturation. The samples were fixed among the standing cubes of epoxy resin to enhance the overall performance of the samples and ensured that the experimental surfaces were exposed. Strict surface roughness is a requirement for scanning electron microscope and nanoindentation experiments. Firstly, the samples were carefully polished to a surface roughness of 0.5 mm using different grit sizes of 180#–4000# (180, 400, 1000, 2000, 2500, 4000) abrasive paper turn. The sample surfaces were then continuously polished for 2 h using a high energy argon ion beam (Leica EM RES 102) under vacuum conditions, alternating 5 kV and 2 kV voltages, a polishing angle of 4.5°, and a current of 2 mA. After polishing, the sample surfaces were cleaned using high-pressure gas. The roughness of the polished surfaces of the two shale samples was tested by Atomic Force Microscope (AFM), and the results showed that the roughness was controlled between 30 nm and 60 nm for both samples.

2.2. Experimental methods and design

The microstructures of Longmaxi marine shale and Qingshankou continental shale were characterized using XRD analysis, FE-SEM with mineral analysis system, FIB, and python post-processing. The effect of microstructure difference on mechanical properties was quantitatively analyzed by nanoindentation experiments based on typical shale bedding layers marked by FIB. Finally, the bedding fractures distribution patterns of the two types of shales were then established based on the aforementioned findings.

XRD is the primary method for studying the physical phase and crystal structure of the material. The remaining part of the sample was ground into 10–20 g powder, 200 mesh, with dry and homogeneous grains. Using XRD measurements, the mineral composition of the two shales was determined by using the Chinese Oil and Gas Industry Standard SY/T 5163-2010.

The surface morphology and mineralogy of selected areas of both shale types were determined by using FE-SEM with mineral analysis system. Utilizing the Atlas 5 system, a wide variety of high-resolution images were obtained. This system, unlike conventional methods, is based on EDS and can create millimeter-scale image stitching of dozens of images of adjacent areas on the same sample, while ensuring that the acquired images are clear and sharp and that the mineral distribution rather than the elemental distribution in the plane of the scanned area can be obtained. Fixing the sample with double-sided carbon conductive tape before the experiment not only substantially reduces the X-ray value of the background, but also improves the observation accuracy. The accelerating voltage is 10 kV and the emission current is 5 nA.

FIB is a technique that uses a strong current ion beam to exfoliate surface atoms, thereby producing nanoscale surface morphology on the sample surface. SEM images of the entire sample were used to identify typical shale bedding layers area. A pit of 15 μm length, 10 μm width, and 10 μm depth was made at the upper and lower limits of the selected area using the FIB, thereby assuring accurate positioning for SEM and nanoindentation mechanical tests (Fig. 2).

Nanoindentation is characterized by a computer-controlled continuous load variation and online monitoring of indentation depth. A complete indentation process consists of two steps, the so-called loading process, and the unloading process. In the loading process, an external load is applied to the indenter to press into the sample surface. As the load increases, the depth of indentation into the sample increases, and when the load reaches the maximum value, the external load is removed, leaving a residual indentation mark on the sample surface. Fig. 3(a) shows a typical load-displacement curve.

Continuous Stiffness Measurement (CSM) has been selected to measure the mechanical properties in typical shale bedding layers. The CSM was used to determine the elastic contact stiffness of the interface with a constant frequency sinusoidal dynamic loading, and then a continuous small-scale elastic loading-unloading process of the interface was performed to calculate the hardness and

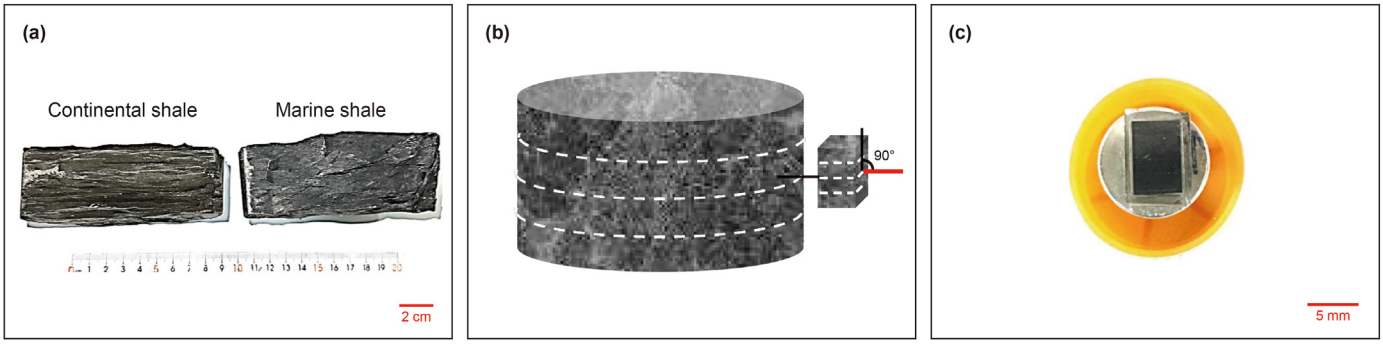

Fig. 1. Shale sample preparation process: **(a)** marine and continental downhole cores; **(b)** sampling diagram for nanoindentation test; **(c)** polished shale sample.

Young's modulus at different depths or loads (Oliver and Pharr, 1992):

$$H = \frac{P_{\max}}{A_c} \tag{1}$$

$$A_c = 24.56\, h_c^2 + C h_c \tag{2}$$

$$h_c = h_{\max} - 0.75 \times \frac{P_{\max}}{S} \tag{3}$$

$$S = \left.\frac{dP}{dh}\right|_{h=h_{\max}} \tag{4}$$

where H is the hardness, $P_{\max}$ is the peak of the loading stage, $h_{\max}$ is the maximum depth, S is the contact stiffness calculated from the initial slope of the unloading stage, and C is the calibrated constant.

$$\frac{1}{E_r} = \frac{(1-\nu)^2}{E} + \frac{(1-\nu_i)^2}{E_i} \tag{5}$$

$$E_r = \frac{\sqrt{\pi}}{2}\frac{S}{\sqrt{A_c}} \tag{6}$$

where E and ν are Young's modulus and Poisson's ratio of the sample, respectively, and E_i and ν_i are Young's modulus and Poisson's ratio of the indenter.

The Keysight Nanoindenter G200 was used to conduct nanoindentation experiments on the selected areas. The nanoindentation points were located on the vertical bisector at the upper and lower FIB marks of each layer. Shale is a typical heterogeneous rock composed of hard brittle minerals like quartz and feldspar, in addition to clay minerals (Mokhtari et al., 2016). To ensure that the results accurately reflect the mechanical properties of the shale, the number of points per layer is set at 15 with a spacing of 100 μm to eliminate the interference of adjacent indentation points. The indenter is a Berkovich diamond indenter with a wide range of spring constants, the indenter direction is perpendicular to the bedding plane direction and the indentation depth is set at 3000 nm to ensure that the indentation depth contains as many minerals as possible. A constant loading strain rate of 0.05 s^{-1} and a frequency of 45 Hz were ensured for the indenter, and all experiments were conducted at room temperature. Fig. 3(b) shows a schematic diagram of the nanoindentation test scheme for the selected area.

3. Results

3.1. Relationship between sedimentary environment and shale microstructure

Table 1 illustrates the mineral composition of the shales in two different sedimentary environments tested by XRD. The results show that both types of shales are predominantly clay-rich, with 57.92% clay content in the Longmaxi marine shale and 51.59% clay content in the Qingshankou continental shale. The siliceous and carbonate mineral contents of Longmaxi marine shale were 34.08% and 3.61%, respectively, while the siliceous and carbonate mineral contents of the Qingshankou continental shale were 39.56% and 5.6%, respectively.

Based on the obtained mineral distribution images, the grain size differences of hard brittle minerals other than clay minerals in the two types of shales were further quantified and compared. The 776 μm × 753 μm areas around the fractures were selected in the mineral distribution images of marine shale and continental shale, respectively, and the grain size information of hard brittle minerals in the selected area was calculated using the CV image processing database in python for both types of shales. The mineral extraction process is shown in Fig. 4. The Opencv findContours function was used to retrieve contours from the image to extract closed areas of all hard brittle minerals from the two types of shale mineral distribution images. The Opencv contourArea function was used to calculate the size of the area of the identified closed area and thus obtain the proportion of the area of the selected area occupied by different grain sizes of hard brittle minerals. The equivalent grain size is defined as half the length of the diagonal of the smallest outer rectangle of each hard brittle mineral closure:

$$R = \frac{\sqrt{a^2 + b^2}}{2} \tag{7}$$

where R is the equivalent grain size of the hard brittle mineral, and a and b are the length and width of the minimum external rectangle, respectively.

The percentage of hard brittle minerals with different grain sizes at 5 μm intervals is shown in Fig. 5. The grain size of hard brittle minerals in both types of shales are mainly larger than 20 μm, but there are significantly more brittle minerals with grain sizes larger than 20 μm in Qingshankou continental shale than in Longmaxi marine shale. On the contrary, hard brittle minerals with grain sizes smaller than 20 μm are predominant in Longmaxi marine shale.

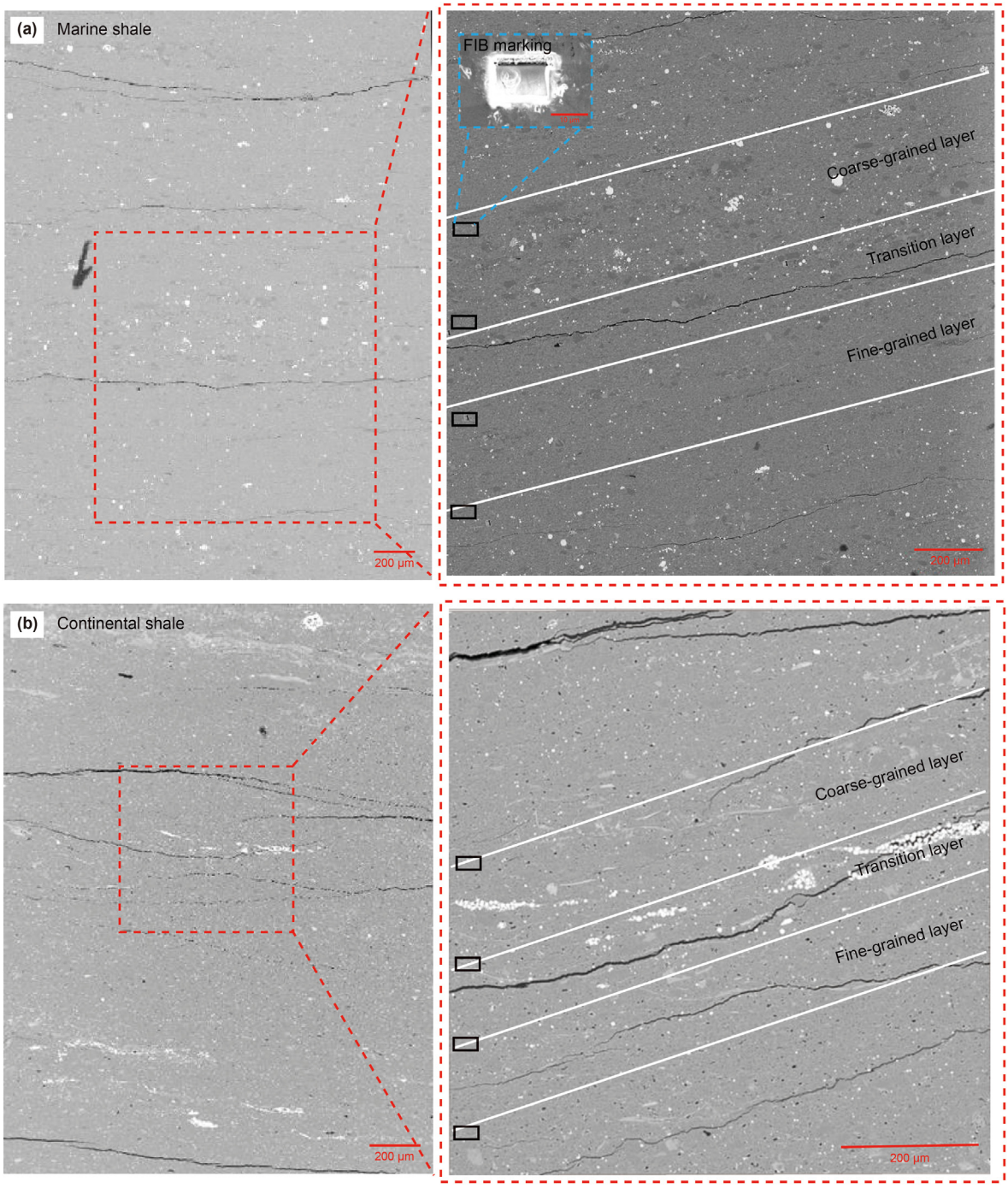

Fig. 2. Typical shale bedding layer areas of **(a)** Longmaxi marine shale and **(b)** Qingshankou continental shale.

3.2. Effects of microstructure on mechanical properties by nanoindentation

The load-displacement curves are the basis for the subsequent analysis of the results of the mechanical parameter tests. The load-displacement curves of shales with various microstructures investigated by nanoindentation are shown in Fig. 6. It can be seen that the load-displacement curves of the Longmaxi marine shale are more densely distributed, with the load variation range of 135–385 mN at an indentation depth of 3000 nm, while the load-displacement curves of the Qingshankou continental shale are relatively dispersed, with the load variation range of 140–840 mN at an indentation depth of 3000 nm. It indicates that the Longmaxi marine shale exhibits a comparatively homogeneous mechanical response at a given indentation depth, while the large-scale distribution of loads in the Qingshankou continental shale indicates its strong heterogeneity.

The "pop-in" phenomenon of sudden displacement jumps was observed in the loading phase of the load-displacement curves in both this and previous studies (Shi et al., 2019; Wang et al., 2022). It is due to the strong heterogeneity of the shale, which leads to increasing local strain energy of the rock as the indenter penetrates

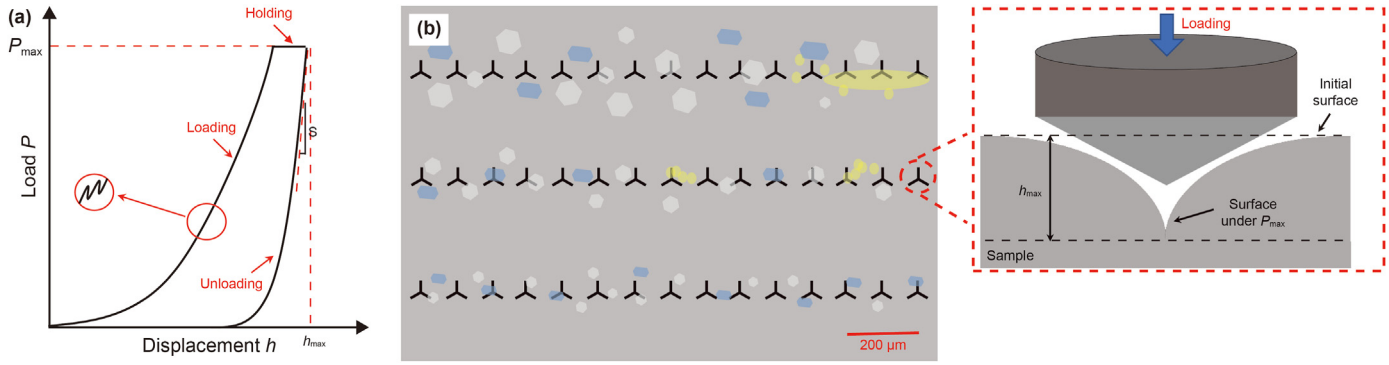

Fig. 3. Schematic diagram of **(a)** nanoindentation load-displacement curve under the CSM mode and **(b)** nanoindentation test scheme.

Table 1
Mineral composition of shale samples.

Sample	Composition, wt%						
	Quartz	Clay	Feldspar	Pyrite	Calcite	Dolomite	Others
Marine shale	26.56	57.92	7.52	2.64	0.3	0.67	4.39
Continental shale	23.96	51.59	15.6	4.15	1.24	0.21	3.25

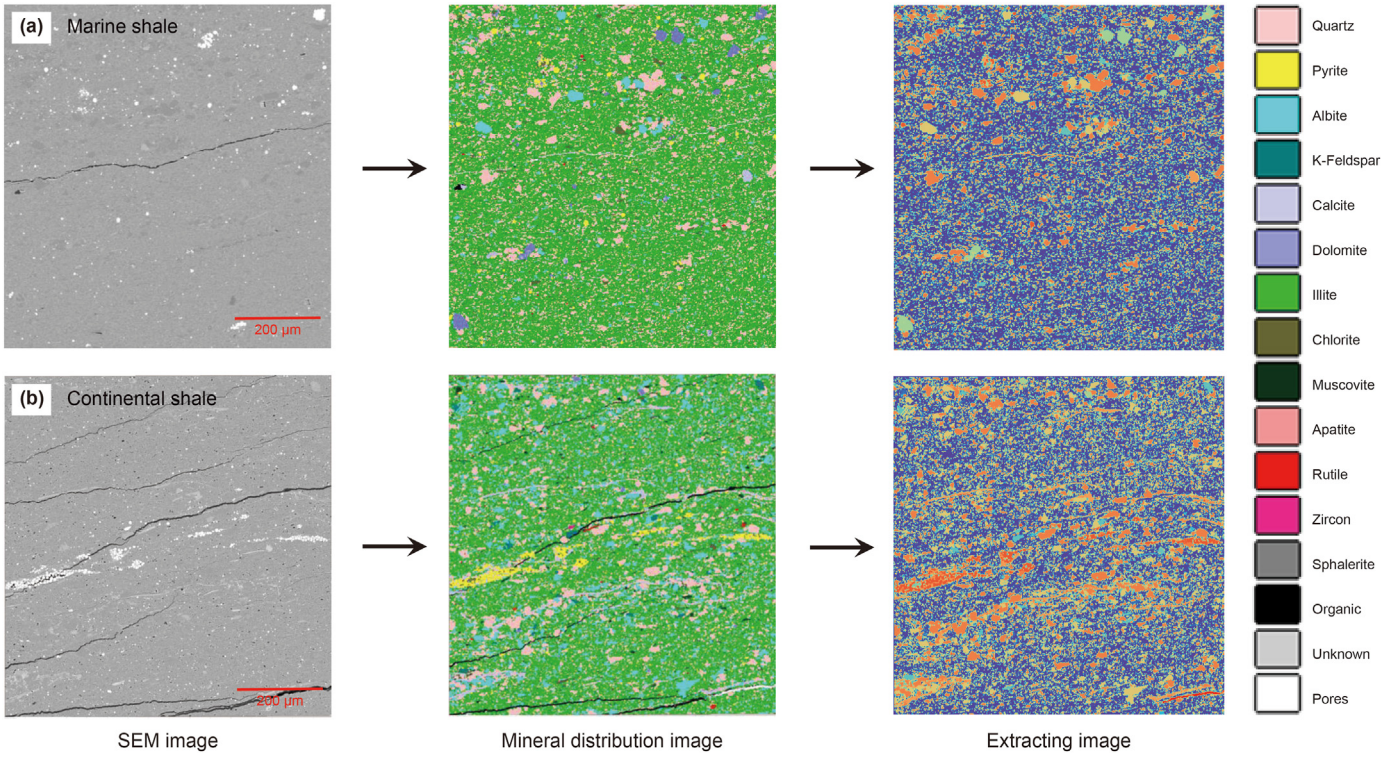

Fig. 4. Mineral extraction process of **(a)** Longmaxi marine shale and **(b)** Qingshankou continental shale.

deeper, and when a critical value is reached, the fractures generated by the nanoindentation meet with the pores, microcracks, and other mechanically weaker materials inside the shale. It can be seen from Fig. 6 that the load-displacement curves of the Longmaxi marine shale are more continuous in the loading phase, with only a very small portion of "pop-in" phenomena, while more "pop-in" phenomena can be observed in the load-displacement curves of the Qingshankou continental shale.

The indentation morphology of the two types of shales also differs greatly, and Fig. 7 illustrates the typical indentation morphology of Longmaxi marine shale and Qingshankou continental shale. It can be found that when the indentation depth is consistent, the indentation morphology of the Longmaxi marine shale is more regular and uniform in size. The indentation morphology of the Qingshankou continental shale is more heterogeneous and of different sizes, and a large number of irregular cracks and protrusions are generated around the indentation.

Fig. 8 shows the curves of hardness and Young's modulus versus

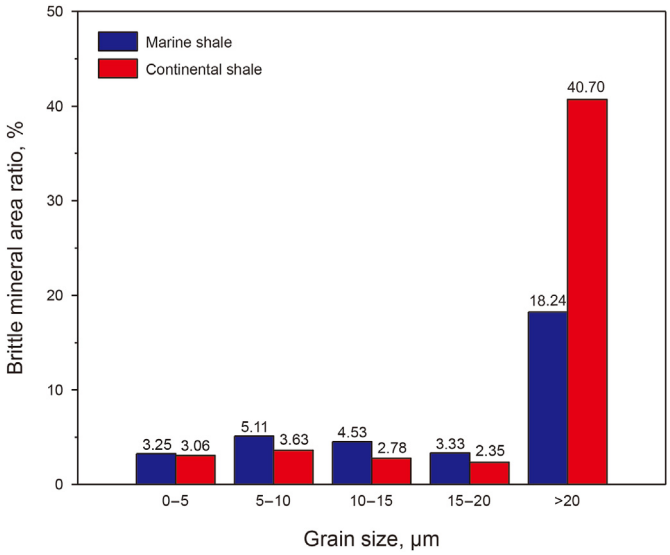

Fig. 5. Proportion of hard brittle minerals with different grain sizes.

indentation depth for all indentation points of the two types of shales. The results demonstrate that when the indentation depth is in the range of 0–2500 nm, the hardness and Young's modulus curves of each indentation point exhibit different degrees of fluctuation with the depth of the indenter. When the indentation depth exceeds 2500 nm, the fluctuation degree progressively converges to a smaller range. It is because the area initially contacted by the indenter contains fewer mineral species, and as the indenter gradually penetrates the shale, more minerals are contacted, and the final convergence of the curves indicates that the indentation area already contains a complete mineral cluster unit (Luo et al., 2020).

The average values of the hardness and modulus of all indentation points at an indentation depth of 3000 nm were calculated separately for the two types of shales, and the results are shown in Fig. 9. The average hardness of the Longmaxi marine shale is 1.29 GPa and the average modulus is 50.93 GPa. The average hardness of the Qingshankou continental shale is 1.7 GPa and the average modulus is 51.5 GPa. The results show that the average hardness and modulus of the Qingshankou continental shale are larger than Longmaxi marine shale.

3.3. Effects of microstructure on bedding fractures distribution

The characteristics of bedding fracture distribution are revealed by observing the microstructure of shale in two different sedimentary environments. As illustrated in Fig. 4, fractures extend along the bedding plane and distribute discontinuously in parallel within the same microscopic scale. The bedding fracture density of

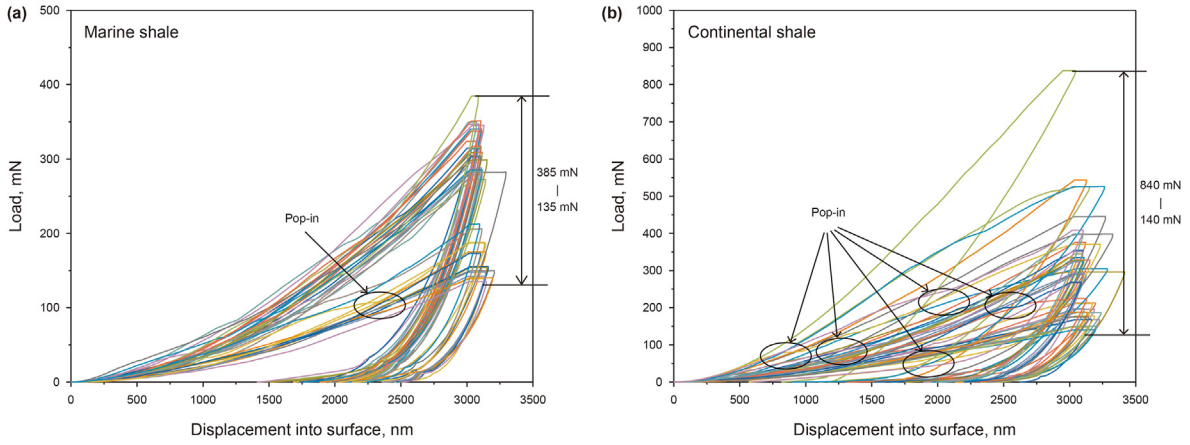

Fig. 6. Load-displacement curves of **(a)** Longmaxi marine shale and **(b)** Qingshankou continental shale.

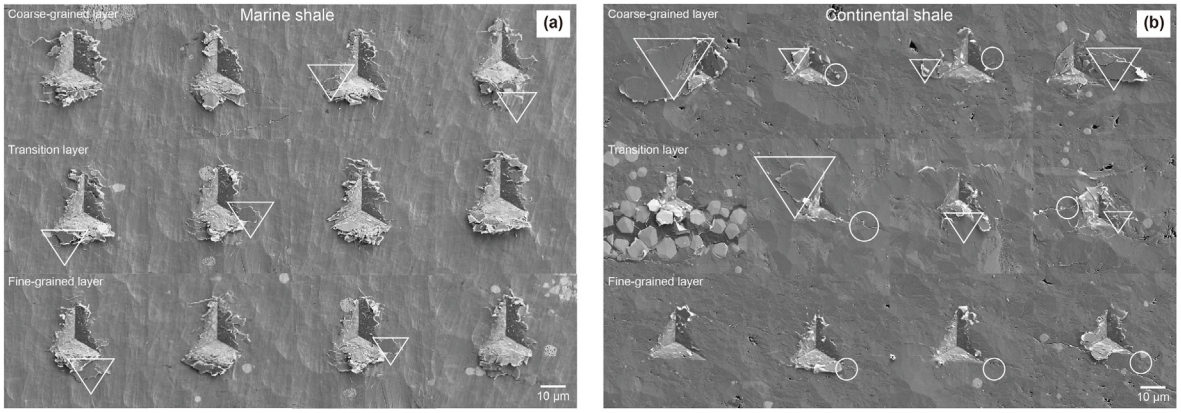

Fig. 7. Microscopic indentation morphology of **(a)** Longmaxi marine shale and **(b)** Qingshankou continental shale (the ellipse region and the triangle region are the irregular cracks and protrusions caused by indentation, respectively).

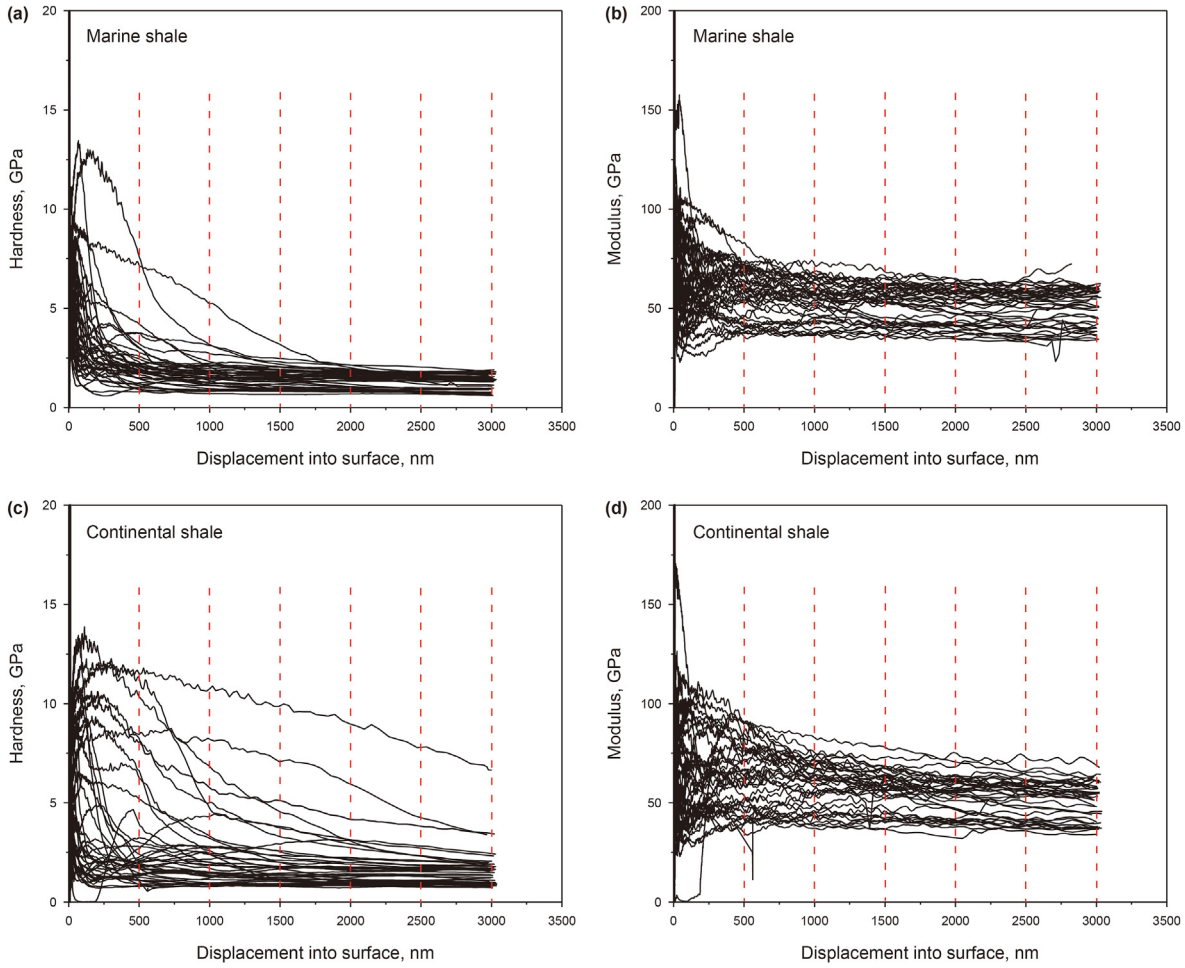

Fig. 8. CSM hardness and modulus curves of each indentation point in ((**a**), (**b**)) Longmaxi marine shale and ((**c**), (**d**)) Qingshankou continental shale.

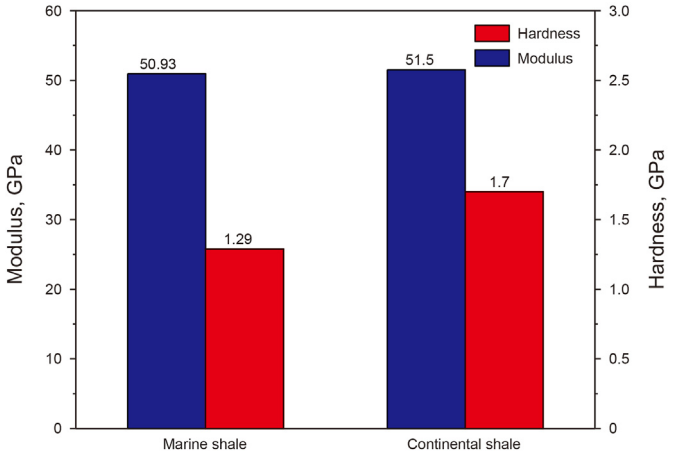

Fig. 9. Average hardness and modulus of Longmaxi marine shale and Qingshankou continental shale.

Qingshankou continental shale is 11.6 strips/mm, and the bedding fracture density of Longmaxi marine shale is 4.1 strips/mm. The fracture density of Qingshankou continental shale is much higher than Longmaxi marine shale. The hard brittle minerals in both types of shales have a large amount of layered distribution. The fractures that encounter hard mineral grains such as quartz and feldspar in the extension process will bypass along their edges and are more likely to develop in the clay mineral layers around hard brittle minerals (Fig. 10) (Liu et al., 2022a).

In order to further clarify the bedding fractures distribution, the proportion of hard brittle minerals in the selected individual layer of typical areas and the proportion of hard brittle minerals with large grain size (>20 μm) were calculated separately based on the aforementioned python processing method. The results are displayed in Fig. 11. The proportion of hard brittle minerals in each individual layer of Longmaxi marine shale are 38.12%, 37.85%, and 33.64%, respectively, and the proportion of large-grained hard brittle minerals are 22.56%, 21.69%, and 13.87%, respectively. The proportion of hard brittle minerals in each individual layer of Qingshankou continental shale is 58.37%, 49.82%, and 45.06%, while the proportion of large-grained hard brittle minerals are 55.91%, 43.76%, and 34.69%, respectively. Therefore, the selected typical areas can be defined as coarse-grained layers, transition layers, and fine-grained layers, respectively.

Fig. 12 illustrates the mechanical properties of each individual layer in the selected areas. The average modulus and hardness were calculated in Fig. 13 for each point of each individual layer along the depth of 2500–3000 nm with a step length of 100 nm. The results show that each layer's modulus and hardness relationships are as follows: coarse-grained layer > transition layer > fine-grained layer. For Longmaxi marine shale, the hardness of the coarse-grained layer is about 19.83% higher than the transition layer and about 22.88% higher than the fine-grained layer. The modulus of the

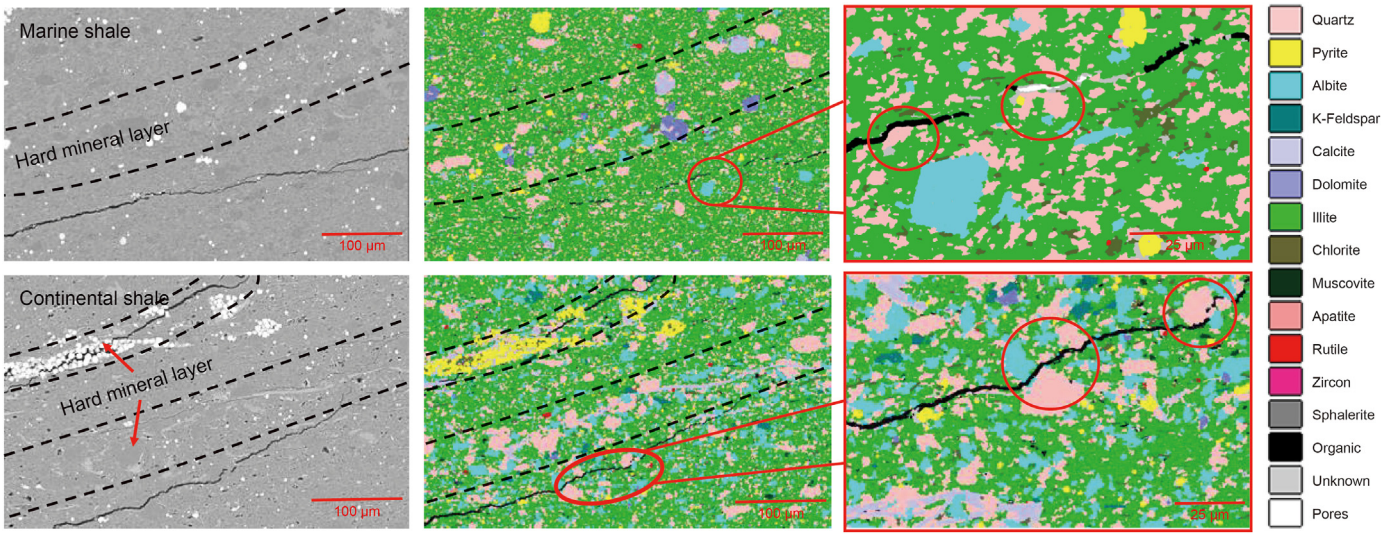

Fig. 10. Characteristics of mineral differentiation and bedding fracture development in laminated shales (red circles show the phenomenon that the fractures encounter hard mineral grains detour).

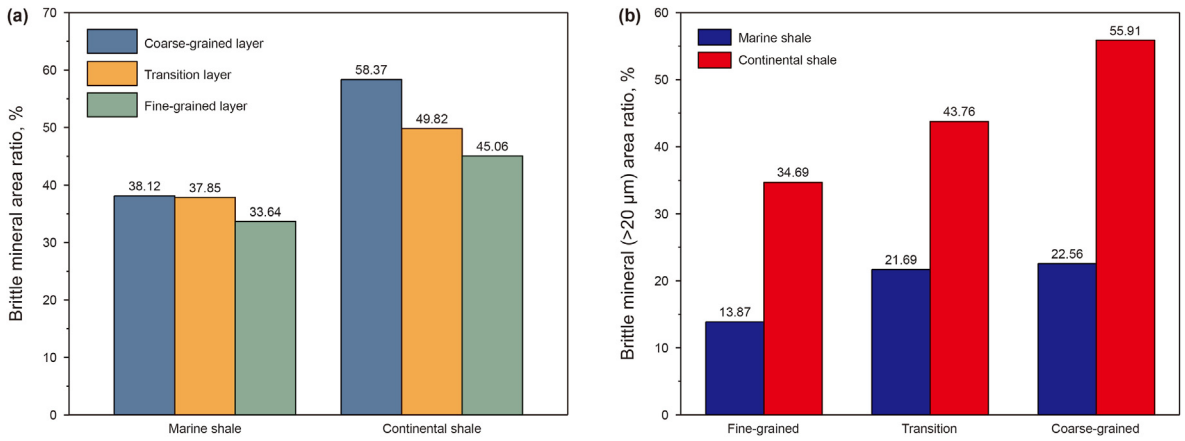

Fig. 11. Proportion of **(a)** hard brittle minerals and **(b)** hard brittle minerals with large grain size (>20 μm) in the selected each individual layer of typical areas.

coarse-grained layer is about 6.59% higher than the transition layer, and about 8.76% higher than the fine-grained layer. For Qingshankou continental shale, the hardness of the coarse-grained layer is about 25.15% higher than the transition layer and about 38.05% higher than the fine-grained layer. The modulus of the coarse-grained layer is about 5.87% higher than the transition layer, and about 8.85% higher than the fine-grained layer. The bedding fractures are located precisely in the transition region where the coarse-grained layer meets the fine-grained layer.

4. Discussion

The differences in microstructure and mechanical properties between marine shale of the Lower Silurian Longmaxi Formation and continental shale of the Upper Cretaceous Qingshankou Formation have been investigated and their effects on bedding fractures distribution have been evaluated in this study. The mineral composition and grain size distribution are the main factors affecting the microstructure of the shale. The XRD test results indicate that there are significant differences in mineral composition between marine shale and continental shale. Overall, the clay mineral content of both shale types is dominant, but the clay mineral content of marine shale is higher and the hard brittle mineral content is lower, particularly feldspar mineral. Python processing results show that the average grain size of marine shale is smaller than continental shale, which is the same as the previous experimental results of Xiao et al. (2021). It indicates that Longmaxi marine shale sample is dominated by fine-grained and clay mineral grains and Qingshankou continental shale sample is dominated by coarse-grained and hard mineral grains.

The nanoindentation mechanical tests further reveal the heterogeneity of the shale and confirm the relationship between microstructure and mechanical properties. The large number of "pop-in" phenomena in the load-displacement curves and the complex indentation patterns of the continental shale sample indicate higher brittleness (Lu et al., 2022). In addition to the above two types of shale samples, the main minerals in the shale were selected for mechanical properties testing, and the specific values are shown in the Appendix. The results show that the modulus and hardness of different minerals vary substantially, and the specific hardness and modulus relationships are as follows: clay mineral < calcite < feldspar < quartz. The higher feldspar content in the Qingshankou continental shale sample leads to relatively higher hardness and modulus, while the higher clay mineral

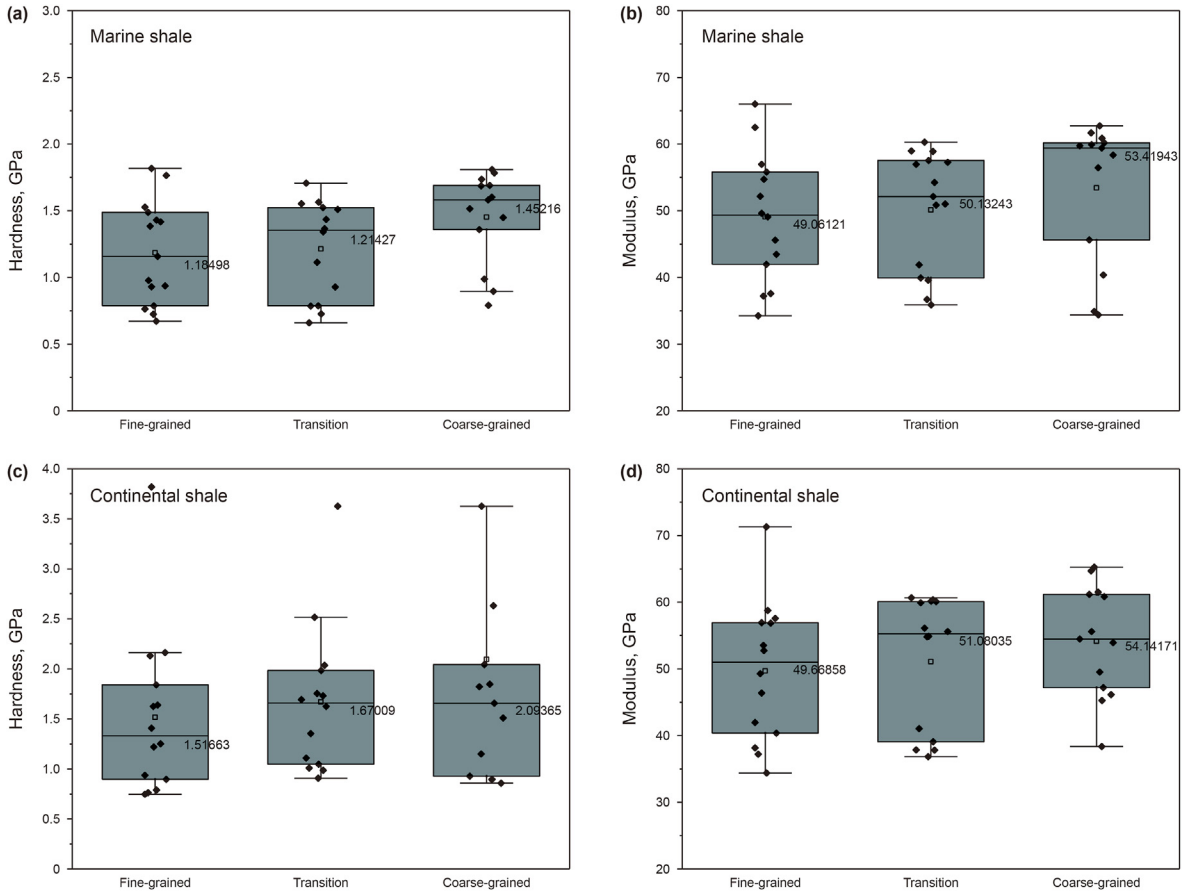

Fig. 12. Mechanical properties of each individual layer in the selected areas.

content in the Longmaxi marine shale sample leads to relatively lower hardness and modulus. The variations in the mechanical properties of the shales are a comprehensive reflection of the different mineral arrangements within them (Shi et al., 2019).

The different sedimentary environment is a crucial factor for the difference in bedding plane density between marine shale and continental shale. The comparison of downhole core profile results between the two types of shale reveals that the bedding plane density of marine shale is much less than continental shale. The average single-layer thickness of Longmaxi marine shale is 1.3 mm and the average single-layer thickness of Qingshankou continental shale is 0.7 mm, which is due to the high frequency of lake-in-lake-out hydrodynamic environment during the deposition of continental shale that would split the shale vertically and make its single layer thickness smaller (Jin et al., 2021). Despite the different bedding plane densities in the two types of shales, nanoindentation mechanical tests based on typical shale bedding layers show that the two types of shales possess similar bedding fracture distribution patterns. The laminated shales are gradually formed by alternating coarse-grained and fine-grained layers during deposition (Cheng et al., 2021), and the bedding fractures are prone to occur in the transition zone from coarse-grained to fine-grained layers of deposition. The fracture orientation is usually parallel to the bedding plane and the fracture bypasses hard brittle grains during the extension process. Therefore, the bedding fracture distribution conjecture as shown in Fig. 14 is proposed. The bedding fracture distribution is influenced by mineral distribution and the weak bedding planes. When the content of hard brittle minerals or clay minerals is low, the fracture extension is difficult. In particular, fractures may be more likely to arise where the clay minerals and hard brittle minerals are more equitably distributed. The stronger heterogeneity of continental shale results in a greater density of bedding fracture distribution, which will affect the degree of effective longitudinal connectivity between hydraulic fractures and the reservoir during hydraulic fracturing (Huo et al., 2021). Meanwhile, strong heterogeneity also plays an important role in the differential enrichment of crude oil in shale reservoirs. Wang et al. (2020b) found that the capillary force has controlling influence on oil accumulation in strongly heterogeneous media and established a criterion to assess the effectiveness of tight reservoirs. Therefore, the geological conditions of the reservoir in the research block should be completely considered in the fracturing design, and the effective reservoirs and petroleum enriched layers should be identified to optimize the scale of fracturing. This is crucial for the effective development of shale reservoirs.

5. Conclusions

The microstructure and mechanical properties of marine shale of the Lower Silurian Longmaxi Formation and continental shale of the Upper Cretaceous Qingshankou Formation were studied by XRD, SEM, and nanoindentation. The bedding fractures distribution was explored in combination with the laminar structure and mineral differentiation features in the two types of shales. The main conclusions of this study are as follows:

(1) The sedimentary environment determines the shale microstructure, and differences in mineral composition and grain

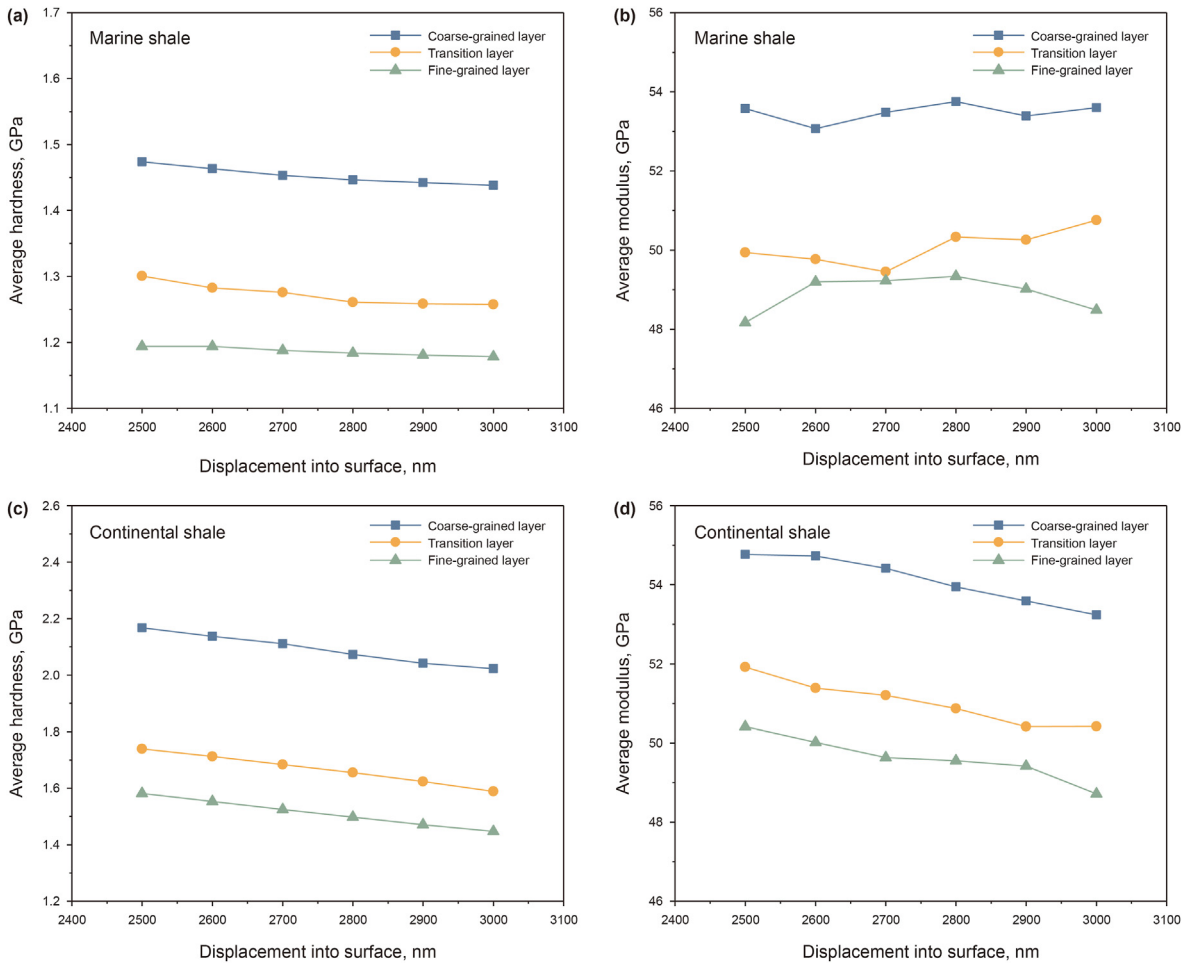

Fig. 13. Average hardness vs. indentation depth and average modulus vs. indentation depth of each individual layer (2500–3000 nm).

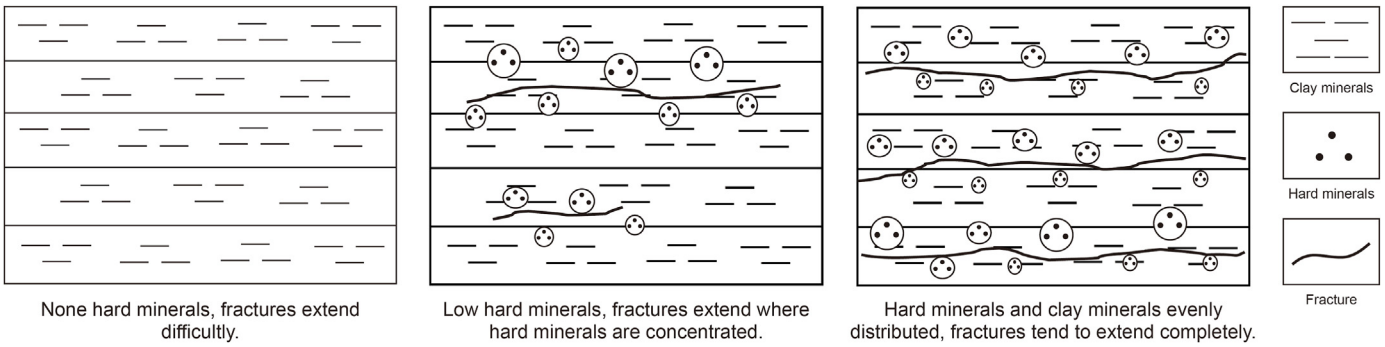

Fig. 14. Schematic diagram of bedding fracture distribution in laminated shale.

size distribution are important factors affecting the microstructure. The Longmaxi marine shale sample is predominantly composed of fine-grained, clay mineral grains, whereas the Qingshankou continental shale sample is predominantly composed of coarse-grained, hard brittle mineral grains.

(2) The shale microstructure leads to the difference in mechanical properties, which is a comprehensive reflection of the different arrangements of minerals in shale. The modulus and hardness of Longmaxi marine shale sample are smaller than Qingshankou continental shale sample. The results of nanoindentation indicate that the mechanical response of Longmaxi marine shale is significantly more uniform than that of Qingshankou continental shale.

(3) The bedding fractures distribution is governed by the laminar structure and mineral arrangement. Shale is composed of hard brittle mineral layers such as large-grained quartz, feldspar, and calcite crossed with soft mineral layers such as clay minerals. The average single-layer thickness of Longmaxi marine shale sample is greater than Qingshankou continental shale sample. During extension, bedding fractures typically develop in the transition layer between

coarse-grained and fine-grained layers and bypass hard brittle mineral grains. The strong heterogeneity of continental shales results in a higher distribution density of bedding fractures.

Declaration of competing interest

The authors declare that they have no known competing financial interests or personal relationships that could have appeared to influence the work reported in this paper.

Acknowledgments

This work was financially supported by the National Natural Science Foundation of China (Grant Nos. 52074315 & U19B6003).

Appendix

Table A1
Mechanical result of the main minerals in the shale

	Hardness, GPa	Modulus, GPa
Quartz	13.15	112.21
Feldspar	8.84	87.23
Calcite	1.96	78.17
Clay mineral	0.12	3.65

References

Cao, H., Gao, Q., Ye, G.Q., Zhu, H.L., Sun, P.H., 2020. Experimental investigation on anisotropic characteristics of marine shale in Northwestern Hunan, China. J. Nat. Gas Sci. Eng. 81, 103421. https://doi.org/10.1016/j.jngse.2020.103421.

Chen, L., Jiang, Z.X., Liu, Q.X., Jiang, S., Liu, K.Y., Tan, J.Q., Gao, F.L., 2019. Mechanism of shale gas occurrence: insights from comparative study on pore structures of marine and lacustrine shales. Mar. Petrol. Geol. 104, 200–216. https://doi.org/10.1016/j.marpetgeo.2019.03.027.

Chen, P., Han, Q., Ma, T.S., Lin, D., 2015. The mechanical properties of shale based on micro-indentation test. Petrol. Explor. Dev. 42, 723–732. https://doi.org/10.1016/S1876-3804(15)30069-0.

Cheng, S.Z., Sheng, M., Chen, Z.W., Tian, S.C., Li, G.S., 2021. Identification of shale bedding layers from micromechanical evaluation. In: SPE Annual Technical Conference and Exhibition. 21–23, September. UAE, Dubai. https://doi.org/10.2118/206256-MS.

Ding, P.B., Gong, F., Zhang, F., Li, X.Y., 2021. A physical model study of shale seismic responses and anisotropic inversion. Petrol. Sci. 18, 1059–1068. https://doi.org/10.1016/j.petsci.2021.01.001.

Dong, G.J., Chen, P., 2017. A comparative experiment investigate of strength parameters for Longmaxi shale at the macro-and mesoscales. Int. J. Hydrogen Energy 42, 20082–20091. https://doi.org/10.1016/j.ijhydene.2017.05.240.

Gong, F., Di, B.R., Wei, J.X., Ding, P.B., Pan, X., Zu, S.H., 2018. Ultrasonic velocity and mechanical anisotropy of synthetic shale with different types of clay minerals. Geophysics 83, MR57–MR66. https://doi.org/10.1190/geo2016-0590.1.

Huo, Z.P., Gao, J.B., Zhang, J.C., Zhang, D., Liang, Y.T., 2021. Role of overlying and underlying limestones in the natural hydraulic fracturing of shale sections: the case of marine–continental transitional facies in the Southern North China Basin. Energy Rep. 7, 8711–8729. https://doi.org/10.1016/j.egyr.2021.11.025.

Huo, Z.P., Zhang, J.C., Li, P., Tang, X., Yang, X., Qiu, Q.L., Dong, Z., Li, Z., 2018. An improved evaluation method for the brittleness index of shale and its application—a case study from the southern north China basin. J. Nat. Gas Sci. Eng. 59, 47–55. https://doi.org/10.1016/j.jngse.2018.08.014.

Jia, Y.Z., Tang, J.R., Lu, Y.Y., Lu, Z.H., 2021. Laboratory geomechanical and petrophysical characterization of Longmaxi shale properties in Lower Silurian Formation, China. Mar. Petrol. Geol. 124, 104800. https://doi.org/10.1016/j.marpetgeo.2020.104800.

Jiang, S., Tang, X.L., Cai, D.S., Xue, G., He, Z.L., Long, S.X., Peng, Y.M., Gao, B., Xu, Z.Y., Dahdah, N., 2016. Comparison of marine, transitional, and lacustrine shales: a case study from the Sichuan Basin in China. J. Pet. Sci. Eng. 150, 334–347. https://doi.org/10.1016/j.petrol.2016.12.014.

Jin, Z.J., Wang, G.P., Liu, G.X., Gao, B., Liu, Q.Y., Wang, H.L., Liang, X.P., Wang, R.X., 2021. Research progress and key scientific issues of continental shale oil in China. Acta Pet. Sin. 42, 821. https://doi.org/10.7623/syxb202107001.

Lawal, L.O., Mahmoud, M., Adebayo, A., Sultan, A., 2021. Brittleness and microcracks: a new approach of brittleness characterization for shale fracking. J. Nat. Gas Sci. Eng. 87, 103793. https://doi.org/10.1016/j.jngse.2020.103793.

Li, N., Jin, Z.J., Wang, H.B., Zou, Y.S., Zhang, S.C., Li, F.X., Zhou, T., Jiang, M.Q., 2023. Investigation into shale softening induced by water/CO_2-rock interaction. Int. J. Rock Mech. Min. Sci. 161, 105299. https://doi.org/10.1016/j.ijrmms.2022.105299.

Li, Q.W., Pang, X.Q., Tang, L., Chen, G., Shao, X.H., Jia, N., 2018. Occurrence features and gas content analysis of marine and continental shales: a comparative study of Longmaxi Formation and Yanchang Formation. J. Nat. Gas Sci. Eng. 56, 504–522. https://doi.org/10.1016/j.jngse.2018.06.019.

Li, W.F., Wang, X.Y., Cheng, J.Y., 2019. Measurement of the anisotropic elastic properties of shale: uncertainty analysis and water effect. Bull. Eng. Geol. Environ. 78, 6075–6087. https://doi.org/10.1007/s10064-019-01517-y.

Liu, K.Q., Ostadhassan, M., Bubach, B., 2016. Applications of nano-indentation methods to estimate nanoscale mechanical properties of shale reservoir rocks. J. Nat. Gas Sci. Eng. 35, 1310–1319. https://doi.org/10.1016/j.jngse.2016.09.068.

Liu, X., Meng, S.W., Liang, Z.Z., Tang, C.A., Tao, J.P., Tang, J.Z., 2022a. Microscale crack propagation in shale samples using focused ion beam scanning electron microscopy and three-dimensional numerical modeling. Petrol. Sci. 20, 1488–1512. https://doi.org/10.1016/j.petsci.2022.10.004.

Liu, Y.W., Liu, A., Liu, S.M., Kang, Y., 2022b. Nano-scale mechanical properties of constituent minerals in shales investigated by combined nanoindentation statistical analyses and SEM-EDS-XRD techniques. Int. J. Rock Mech. Min. Sci. 159, 105187. https://doi.org/10.1016/j.ijrmms.2022.105187.

Lu, Y.Y., Cheng, Q., Tang, J.R., Liu, W.C., Li, H.L., Liu, J., Xu, Z.J., Tian, R.R., Sun, X., 2022. Differences in micromechanical properties of shales from different depositional environment: a case study of Longmaxi marine shale and Yanchang continental shale using nanoindentation. J. Nat. Gas Sci. Eng. 107, 104727. https://doi.org/10.1016/j.jngse.2022.104727.

Luo, S.M., Lu, Y.H., Wu, Y.K., Song, J.L., DeGroot, D.J., Jin, Y., Zhang, G.P., 2020. Cross-scale characterization of the elasticity of shales: statistical nanoindentation and data analytics. J. Mech. Phys. Solid. 140, 103945. https://doi.org/10.1016/j.jmps.2020.103945.

Mokhtari, M., Honarpour, M.M., Tutuncu, A.N., Boitnott, G.N., 2016. Characterization of elastic anisotropy in Eagle Ford Shale: impact of heterogeneity and measurement scale. SPE Reservoir Eval. Eng. 19, 429–439. https://doi.org/10.2118/170707-PA.

Oliver, W.C., Pharr, G.M., 1992. An improved technique for determining hardness and elastic modulus using load and displacement sensing indentation experiments. J. Mater. Res. 7, 1564–1583. https://doi.org/10.1557/JMR.1992.1564.

Shi, X., Jiang, S., Lu, S.F., He, Z.L., Li, D.J., Wang, Z.X., Xiao, D.S., 2019. Investigation of mechanical properties of bedded shale by nanoindentation tests: a case study on Lower Silurian Longmaxi Formation of Youyang area in southeast Chongqing, China. Petrol. Explor. Dev. 46, 163–172. https://doi.org/10.1016/S1876-3804(19)30016-3.

Wang, J.F., Yang, C., Liu, Y.K., Xiong, Y.Q., 2022. Nanoindentation investigation of mechanical and creep properties of continental Triassic Yanchang Formation shale, Ordos Basin. Interpretation 10, SJ29–SJ41. https://doi.org/10.1190/INT-2021-0218.1.

Wang, L., Guo, Y.T., Yang, C.H., Xiao, J.L., Lu, C.S., Song, Y.F., 2020a. Mechanical characterization of continental shale in Sichuan Basin of China and its potential impact on reservoir stimulation. J. Nat. Gas Sci. Eng. 79, 103346. https://doi.org/10.1016/j.jngse.2020.103346.

Wang, W.Y., Pang, X.Q., Chen, Z.X., Chen, D.X., Ma, X.H., Zhu, W.P., Zheng, T.Y., Wu, K.L., Zhang, K., Ma, K.Y., 2020b. Improved methods for determining effective sandstone reservoirs and evaluating hydrocarbon enrichment in petroliferous basins. Appl. Energy 261, 114457. https://doi.org/10.1016/j.apenergy.2019.114457.

Wang, W.Y., Pang, X.Q., Chen, Z.X., Chen, D.X., Zheng, T.Y., Luo, B., Li, J., Yu, R., 2019. Quantitative prediction of oil and gas prospects of the Sinian-lower Paleozoic in the Sichuan basin in central China. Energy 174, 861–872. https://doi.org/10.1016/j.energy.2019.03.018.

Wei, Y., Nie, X., Jin, L.D., Zhang, C., Zhang, C.M., Zhang, Z.S., 2018. Investigation of sensitivity of shale elastic properties to rock components based on a digital core technology and finite element method. Arabian J. Geosci. 11, 1–14. https://doi.org/10.1007/s12517-018-3576-5.

Xiao, D.S., Lu, S.F., Shao, M.L., Zhou, N.W., Zhao, R.W., Peng, Y., 2021. Comparison of marine and continental shale gas reservoirs and their gas-bearing properties in China: the examples of the Longmaxi and Shahezi shales. Energy Fuels. 35, 4029–4043. https://doi.org/10.1021/acs.energyfuels.0c04245.

Xie, W.D., Wang, M., Wang, H., Ma, R.Y., Duan, H.Y., 2021. Diagenesis of shale and its control on pore structure, a case study from typical marine, transitional and continental shales. Front. Earth Sci. 15, 378–394. https://doi.org/10.1007/s11707-021-0922-9.

Yang, C.H., Liu, J.J., 2021. Petroleum rock mechanics: an area worthy of focus in geo-energy research. Adv. Geo-Energy Res. 5, 351–352. https://doi.org/10.46690/ager.2021.04.01.

Yang, R., He, S., Hu, Q.H., Zhai, G.Y., Yi, J.Z., Zhang, L., 2018. Comparative investigations on wettability of typical marine, continental, and transitional shales in the middle Yangtze Platform (China). Energy Fuels. 32, 12187–12197. https://doi.org/10.1021/acs.energyfuels.8b02805.